

Nonlinear feedback for control of chaos

M. de Sousa Vieira* and A. J. Lichtenberg

Department of Electrical Engineering and Computer Sciences, University of California, Berkeley, CA 94720, USA.

We generalize a method of control of chaos which uses delayed feedback at the period of an unstable orbit to stabilize that orbit. The generalization consists of substituting some portion of the nonlinear dynamical system with a delayed dynamics, rather than using a linear delay function for control. A further generalization, in which the control function retains memory of all previous periods, allows the region of the parameter space over which control can be achieved to be extended, but at the price of losing the ability to achieve superstability. Nonlinear feedback results in a larger basin of attraction to the stabilized orbit than linear feedback. For a simple test mapping studied (the logistic map) the dimension of the system increases from one to two by introducing control. We show in the case involving memory, for a particular choice of the relationship between the control parameters, that the superstable orbit can be recovered without reducing the parameter space that can be controlled. This particular solution, in addition to having the largest basin of attraction of the methods considered, retains the dimension of the uncontrolled system.

I. INTRODUCTION

A number of methods have been proposed for feedback control of chaos [1–3,5,7]. Two methods of control that stabilize an otherwise unstable periodic orbit have received considerable attention recently:

(a) Ott, Grebogi and Yorke (OGY) [2] introduced a method which stabilizes unstable periodic orbits (UPO's) found in the chaotic regime via small feedback perturbations to an accessible parameter. The control perturbation is given when the orbit crosses a given Poincaré section, such that the trajectory will be close to the stable manifold of the desired UPO. In this method, in the limit of zero noise, the orbit of the controlled system is identical to the UPO of the uncontrolled system and the feedback perturbation vanishes. A drawback for the OGY method is that it becomes difficult to apply for very fast systems, since it requires computer analysis of the system at each crossing of the Poincaré section. Also, noise can result in occasional bursts where the trajectory wanders far from the controlled periodic orbit.

(b) An alternative method of feedback stabilization of UPO's, introduced by Pyragas [3], consists of a continuous linear feedback applied at each computational time step. As in the OGY case, in this method the controlled orbit coincides with the UPO of the uncontrolled system

and the feedback vanishes, for zero noise, when control is achieved. The feedback procedure can be applied without knowing a priori the location of the periodic orbit, for a version in which the feedback term contains a delayed variable, in which the delay corresponds to the period of the UPO. Moreover, it is expected that it can be used for fast systems, since no parameters are changed on a fast time-scale, and the method does not require a computer analysis of the system. For some systems, the method is robust even in the presence of considerable noise [4]. A disadvantage of Pyragas' method is that it achieves control only over a limited range of the parameter space, i.e., a given orbit will become eventually unstable in the controlled system as the parameters are varied more deeply into the chaotic regime. The use of delayed feedback also increases the dimensionality of the system. Socolar *et. al.* [5] extended the Pyragas method to include, in the control term, memory of all the previous states of the system, and were thereby able to increase the region of the parameter space where control can be achieved. The dimensionality of the system also increased in this method, to the same extent as in the method of Pyragas.

The desirable properties of a control system depend on the application. Here we consider a system with a fixed period UPO which we are attempting to control. The parameters that control the coordinates of the UPO may be slowly varying compared to the UPO period. The system can be considered subject to noise, which may take the system coordinates away from the periodic orbit. In this general situation we may consider the following properties of the control system as desirable: (1) In the neighborhood of the periodic orbit (assumed stably controlled) the actual orbit returns optimally fast to the periodic orbit when perturbed away from it (in the limiting case the orbit is superstable). (2) A slow drift in parameters can be tracked by the control over the largest possible parameter space. (3) In the larger space we (nonlinearly) want the stability to be maintained over the widest range of uncertainty in either the system parameters or the dynamical variables (basin of attraction) caused by noise. (4) In some average sense, we wish to minimize the time required to return to the desired solution from the basin of attraction (in the nonlinear regime).

In the next section we examine these criteria for control of a fixed point of a mapping corresponding to a periodic solution of a continuous system, with a known period. We use the well studied logistic map as the test bed for the study. Here we introduce modifications to the control methods of Pyragas and Socolar, using a nonlinear function in the feedback term. As in the OGY, Pyragas

and Socolar methods, the stabilized orbit is identical to the UPO of the uncontrolled system, and when control is achieved the magnitude of the feedback term vanishes in the absence of noise. First we compare the linear control of Pyragas to an analogous nonlinear control. Next, we compare the case in which memory is introduced into the mapping parameters with case in which memory is introduced into the nonlinear control. In Section III we introduce a special case of nonlinear control with memory, that reduces to a remarkable simple form, whose properties are generally better than the other cases examined. We show that this latter control can be used efficiently to control other periodic points and higher dimensional mappings.

II. COMPARISON OF CONTINUOUS CONTROL METHODS

We start by describing Pyragas' method [3]. He considered a dynamical system that is governed by ordinary differential equations, which are in principle unknown. However, some scalar variable y can be measured as a system output, and the system also has an input available for an external force f . These assumptions can be met by the following model,

$$\frac{dy}{dt} = P(y, \mathbf{x}) + f(t), \quad \frac{d\mathbf{x}}{dt} = \mathbf{Q}(y, \mathbf{x}), \quad (1)$$

where \mathbf{x} describes the remaining variables of the dynamical system which are not available for observation or not of interest. The forcing term disturbs only the variable y , and it is assumed that the system may be in the chaotic regime when the forcing term $f(t)$ is zero.

Pyragas studied two types of forcing. In the first method one determines the UPO y_i of the chaotic attractor from $y(t)$, following well known algorithms [6]. Then one designs an oscillator that has an orbit equal to that of y_i . The forcing term is given in this case by $f(t) = K[y_i(t) - y(t)]$, where K is an empirically adjustable weight of the perturbation. In the other type of forcing considered by Pyragas, the forcing term contains a delayed term of the variable y , namely, $f(t) = K[y(t - \tau) - y(t)]$, where τ is the delay time. If the delay time coincides with period of the i -th UPO then the perturbation $f(t)$ vanishes and $y(t)$ will coincide with UPO, as in the first case. However, in this last case, one does not need to know the UPO, just its period, nor is it necessary to design an external oscillator. [Although Pyragas described his method for the situation in which one knows only a time series, in all the cases he studied the equations that described the system were known.] Here we are concerned with the second method, i.e., the delayed feedback case.

Applying Eq. (1) for the stabilization of a period-one orbit in a one-dimensional mapping $F(x_n)$, we have

$$x_{n+1} = F(x_n) + K[x_n - x_{n-1}]. \quad (2)$$

The controlled system has dimensionality equal to two instead of one for the unperturbed system. The eigenvalues of Eq. (2) are given by expanding it about the equilibrium $x_{n+1} = x_n$ to obtain,

$$\lambda_{1,2} = \frac{F' + K \pm \sqrt{[F' + K]^2 - 4K}}{2}, \quad (3)$$

where $F' \equiv F'(x_f)$ is the derivative of F with respect to x_n at the fixed point x_f .

We illustrate this method of control using the logistic map,

$$x_{n+1} = F(x_n) = 4ax_n(1 - x_n). \quad (4)$$

This map presents a sequence of period doubling bifurcations as a increases and enters into chaos at $a \approx 0.8925$. The period-one orbit is stable from $a = 0$ to $a = 3/4$. The fixed point x_f for the period-one orbit is zero for $0 \leq a < 1/4$ and $x_f = 1 - 1/4a$ for $1/4 < a < 3/4$. If $a < 0$ or $a > 1$, the attractor is unbounded, diverging to infinity. The attractor will also diverge if the initial condition x_0 is not in the interval $[0, 1]$. The period-one orbit loses stability when one of the eigenvalues has modulus larger than one. For the logistic map, for $K < 1$, an eigenvalue crosses -1, causing the appearance of a pitchfork bifurcation. When this occurs, Eq. (3) gives $F'(x_f) = -1 - 2K$. Since, for the logistic map $F'(x_f) = 2 - 4a$, the bifurcation point a^* is

$$a^* = \frac{3 + 2K}{4}. \quad (5)$$

A Hopf bifurcation occurs at $K = 1$, where the eigenvalues cross the unit circle with imaginary values. Beyond this value of K there is no stable solution, so the maximum value of a where control can be achieved is given by $a^* = 1.25$.

We compare these results with the use of a nonlinear rather than a linear function in the feedback term. Thus, the forcing term to stabilize a periodic orbit is given by is a nonlinear function $G(x_n, x_{n-1})$. Obviously, many choices can be made for G , with the constraint that $G = 0$ in the desired UPO. Perhaps the simplest construction is $G = -K[F(x_n) - F(x_{n-1})]$, with $K > 0$, since with this feedback one does not need to know the equation $F(x_n)$ that governs the system. We show how this control could be applied in the block diagram displayed in Fig. 1. This feedback also gave a better performance than other nonlinear functions, as discussed below.

For the period-one orbit, our controlled system can be written as

$$x_{n+1} = F(x_n) - K[F(x_n) - F(x_{n-1})]. \quad (6)$$

The eigenvalues for this equation are

$$\lambda_{1,2} = \frac{(1-K)F' \pm \sqrt{[(1-K)F']^2 + 4KF'}}{2}. \quad (7)$$

When a pitchfork bifurcation occurs, for K not very large, the most negative eigenvalue is equal -1 . From Eq. (7) we obtain $F'(x_f) = -1/(1-2K)$. For the logistic map this gives

$$a^* = \frac{3-4K}{4(1-2K)}. \quad (8)$$

From Eq. (8) we see that if $K < 0$, then $a^* < 3/4$. For $K > 1/3$, the period-one loses its stability not via a period doubling bifurcation, but via a Hopf bifurcation. For this case, we obtain

$$a^* = \frac{1+2K}{4K}. \quad (9)$$

With Eqs. (8) and (9) we find that the maximum value for a where control can be achieved with this method is also $a^* = 1.25$, which occurs at $K = 1/3$. We compare a^* as a function of K for the nonlinear control in Fig. 2 (solid line) to that using the linear control of the Pyragas' method (dashed line). In Fig. 3 we compare the values of $\log_2 |\lambda|$, with λ being the least stable eigenvalue, for nonlinear control (solid line) with linear feedback (dashed line) and with no control (short-dashed line). We note that the transient time (in the linear regime), which is proportional to $1/|\log_2 |\lambda||$, is smaller in the nonlinear control than in Pyragas's method. Also, superstable orbit, $\log_2 |\lambda| = -\infty$, is preserved with the nonlinear control. [The reader might well ask why the parameters linearized around the fixed point are not the same for linear and nonlinear control. As pointed out by a referee, the use of a linear (in x) control parameter with $K \rightarrow K(4a-2)$ brings the results into coincidence. However, a dependence of the control on a introduces a new complexity into the feedback, which we consider below]. We note in Fig. 2 that the largest range of stable a , $a < a^*$, occurs at $K = 1$ for the linear control. This has significant disadvantages when we consider the nonlinear phase space, as we now show.

We numerically determined the basin of attraction by constructing a grid of initial conditions in the x_{n-1} , x_n space and determining which are attracted to the fixed point. The effect of noise on the stability is qualitatively examined by constructing a noise circle around the fixed point, which just touches the basin boundary, and finding the radius r of the circle. We illustrate these properties in Fig. 4(a) for the nonlinear control and in Fig. 4(b) for the linear control. In Fig. 5 we show how r varies with a for the nonlinear control at $K = 1/3$ (solid line) and for the linear control along the dotted line of Fig. 2 (dashed line). We see that the nonlinear control is more robust in the presence of noise.

Although the control procedure we have used is straightforward to implement, the reader might well ask

if a different form of nonlinearity might be better. To investigate this possibility we studied the quadratic map

$$x_{n+1} = 1 - ax_n^2. \quad (10)$$

We found that the control term that is most robust in the presence of noise and has the smallest transient is given by $F = Ka(|x_n|^z - |x_{n-1}|^z)$ with $z = 2$.

Another method of control of chaos that follows Pyragas' ideas was introduced by Bielawski *et. al.* [7]. In this method the forcing is given to an accessible *parameter* of the system, instead of adding a feedback term to the equation. The controlled logistic map in this case is given by

$$x_{n+1} = 4(a + \epsilon_n)x_n(1 - x_n), \quad (11)$$

with $\epsilon_n = \frac{K}{4}(x_n - x_{n-1})$. The method has been generalized by Socolar *et. al.* [5], with the controlled logistic map given by Eq. (11), but with

$$\epsilon_n = \frac{K}{4}(x_n - x_{n-1}) + R\epsilon_{n-1}, \quad (12)$$

where $R < 1$. The case $R = 0$ reduces to the Bielawski control. Socolar *et. al.* [5] have shown that this form of the control parameter is equivalent to including memory of all the past states of the system. The dimensionality of the new map is also two with the variables x_n and ϵ_n . The eigenvalues are

$$\lambda_{1,2} = \frac{F' + R + \gamma \pm \sqrt{[F' + R + \gamma]^2 - 4[F'R + \gamma]}}{2}, \quad (13)$$

where $\gamma = K(4a-1)/(4a)^2$. A pitchfork bifurcation occurs at

$$K = 8a^{*2}(R+1)(4a^* - 3)/(4a^* - 1). \quad (14)$$

A Hopf bifurcation occurs at

$$K = 16a^{*2}[1 + 2R(2a^* - 1)]/(4a^* - 1). \quad (15)$$

The stability boundaries $a^*(K, R)$ are given by Eqs. (14) and (15). By varying R one finds that, in the absence of noise, control can be achieved for arbitrary large values of a . However, the width of the window in a where control can be achieved decreases as a increases.

Memory can also be included in the form of nonlinear control by a generalization of Eq. (6),

$$x_{n+1} = F(x_n) + \epsilon_n \quad (16)$$

$$\epsilon_{n+1} = -K[F(x_{n+1}) - F(x_n)] + R\epsilon_n, \quad (17)$$

When $R = 0$ this control reduces to the case of nonlinear control studied above. The eigenvalues are

$$\lambda_{1,2} = \frac{(1-K)F' + R \pm \sqrt{[(1-K)F' + R]^2 + 4(K-R)F'}}{2}, \quad (18)$$

and the stability boundaries for the logistic map are obtained from

$$a^* = \frac{3(1+R) - 4K}{4(1+R) - 8K} \quad (19)$$

for a pitchfork bifurcation, and

$$a^* = \frac{1}{2} + \frac{1}{4(K-R)} \quad (20)$$

for a Hopf bifurcation. The maximum value of a where control can be achieved in this method is $a^* = \frac{5-R}{4(1-R)}$, which occurs at $K = \frac{(R+1)^2}{R+3}$. In Fig. 6 the stability boundaries are shown for the mappings given by Eqs. (16) and (17) (solid line) and Eqs. (11) and (12) (dashed line), with $R = 0.5$. For both mappings, the addition of a memory term (finite R) extends the region in parameter space that a can be tracked. There is a distinct difference in the results of Fig. 6 for the two methods of control. For the Socolar method the range of a that can be stabilized becomes small, as K tracks a to large values. In contrast, the additive nonlinear control picks out a value of K for which the mapping can be controlled for all values of a up to a maximum, and thus is not sensitive to parameter drift or uncertainty. The range of a that can be controlled at the fixed point increases without bound, as $R \rightarrow 1$.

There is a price to pay for having a finite R when the variable is subject to noise. For example, at $R = 0.5$, $a = 1$, $K = 0.6428$ for the additive nonlinear control and $K = 1.8333$ for the parameter control, which correspond, respectively, to the diamond and cross symbols shown in Fig. 6, we numerically find the basin of attraction for the two cases. The result for additive nonlinear control is shown in Fig. 7(a) and for control in the parameter in Fig. 7(b). In both cases the stabilization region has been decreased from that without memory, but much more so with parameter control for which the basin appears to be fractal. The calculation of the noise radius here is somewhat subtle, since ϵ does not have a clear physical meaning. If we add a noise term δx to the right hand side of Eqs. (11) and (12) we note that, when the system is at the fixed point, the variation in x_{n+1} will still be δx . However, the variation in ϵ_{n+1} will be $(1 + \frac{K}{4})\delta x$. If the same procedure is applied to Eqs. (16) and (17) we find that the variation in ϵ_{n+1} will now be $(1 - KF'(x_f))\delta x$. Therefore the noise δx is amplified in the ϵ variable in both cases, with distinct multiplicative factors. To compensate for this, we contract the ϵ coordinate by the respective factor before calculating the noise radius in the basin of attraction of the additive nonlinear control and the parameter control. Our results are shown in Fig. 8 for $R = 0.5$, for nonlinear additive control (solid

line), calculated at $K = 0.6428$, and for parameter control (dashed line), calculated at the median line of the stability boundary shown in Fig. 6. We find that the nonlinear additive control is more robust to noise than the parameter control. However, for the same value of a the nonlinear control with $R > 0$ is less robust than the case with $R = 0$, which is shown in Fig. 5. We must also consider the effect of varying R . We do this only for the case of the additive nonlinear control in the next section.

III. AN OPTIMAL CONTROL FUNCTION

Although, the nonlinear control, with a memory factor R , has a number of desirable properties, there is the drawback that for a given R at the value of K for which a^* obtains its maximum value, there is no superstable orbit (this also occurs in the parameter control). Since operation at a superstable orbit is very desirable from the perspective of return to the fixed point solution in the presence of noise, we look for a relation between K and R for which a superstable orbit is recovered by setting $\lambda = 0$ in Eq. (18). We find two solutions,

$$R = 0, \quad F'(x_f) = 0, \quad (21)$$

that, for the logistic map, corresponds to $a = 0.5$, which is the solution without memory, and

$$R = K, \quad K = \frac{F'(x_f)}{F'(x_f) - 1}, \quad (22)$$

which, for the logistic map, corresponds to $K = \frac{4a-2}{4a-1}$. We call the second solution, Eq. (22), an optimized control function, as it allows operation with superstability, i.e., with maximum control at the fixed point, for $0 \leq a < \infty$. We find that this solution has other desirable properties, such as a large basin of attraction, and, remarkably, *reduces the phase space to a single degree of freedom*.

Substituting $R = K$ into Eq. (17), and eliminating ϵ_n in favor of x_{n+1} by using Eq. (16), we obtain $\epsilon_{n+1} = -K[F(x_{n+1}) - x_{n+1}]$. Dropping the index by 1, and substituting for ϵ_n in Eq. (16), we obtain a remarkably simple form for the mapping equation

$$x_{n+1} = F(x_n) - K[F(x_n) - x_n], \quad (23)$$

which is valid for control of the period-one orbit in one-dimensional maps. At the fixed point, the magnitude of the feedback term vanishes, as in the other methods studied here. A block diagram of the optimal control scheme is shown in Fig. 9. One expects this method to be easy to implement in experiments, since the control term contains only amplified versions of the input and output of the dynamical system and one does not need to know F to apply the control. We note that for the particular

case of a mapping, the period-one orbit is a fixed point. Thus the variable itself can be thought of as a delayed signal at the fundamental period of the updated variable. This property allows us to use a feedback signal with the same index as the mapping function itself. The delayed feedback is seen explicitly for control of differential equations, as discussed below. The eigenvalue for Eq. (23) is given by

$$\lambda = (1 - K)F'(x_f) + K, \quad (24)$$

This map loses stability via a pitchfork bifurcation, where $\lambda = -1$. Consequently, the bifurcation point for the controlled logistic map is at

$$a^* = \frac{3 - K}{4(1 - K)}. \quad (25)$$

Thus, we see that the parameter region where the period-one is stable increases as K increases and tends to infinity as K tends to one.

The superstable orbit, $\lambda = 0$, is obtained at

$$a_s = \frac{2 - K}{4(1 - K)}, \quad (26)$$

where the subscript ‘s’ denotes superstable orbit. Also here a_s increases with K and goes to infinity as K tends to one. In Fig. 10 we show, as a function of K , the values a^* where the period-one bifurcates (solid line) and the values a_s of the superstable orbit (dashed line). We plot in Fig. 11 the Liapunov exponent, $\log_2 |\lambda|$, as a function of a , for $K = 0, 0.4, 0.8$. One can see from this figure that increasing K increases the range of the parameter a around the superstable orbit for which a given transient time can be achieved.

We now calculate the basin of attraction of the controlled UPO. Since our controlled map is one-dimensional this can be found easily. Using Eq. (23) with F given by Eq. (4) the convergence to the UPO will be attained when $0 \leq x_0 \leq 1 + \frac{K}{4a(1-K)}$. Substituting for a at the superstable orbit from Eq. (26) we obtain

$$0 \leq x_0 \leq 1 + \frac{K}{2 - K}. \quad (27)$$

The basin of attraction increases with K , extending from 0 to 1 at $K = 0$ to 0 to 2 at $K = 1$. Since the fixed point is at $x_f = 1 - 1/(4a)$, the noise radius around the fixed point is

$$r = \min \left[1 - \frac{1}{4a}, \frac{K}{4a(1 - K)} + \frac{1}{4a} \right], \quad (28)$$

which, at the superstable orbit, gives

$$r_s = \frac{1}{2 - K}, \quad (29)$$

such that r_s varies from 0.5 to 1 as K varies from 0 to 1. Comparing Eq. (29) to our previous control parameters we see that this optimized control maintains stability better in the presence of noise.

Although the superstable orbit is maintained, it is not clear what happens to the time constant for return to the periodic orbit as, $K \rightarrow 1$, for initial conditions that are started far away from the fixed point. To study the effect of K on the nonlinear transient we do the following: we start the system with 1000 different initial conditions, uniformly distributed in the interval $[0, 1 + \frac{K}{4a(1-K)})$. Then we verify how many iterations on average are necessary to bring the orbit within a radius of 10^{-4} around the fixed point. The result of the nonlinear transient as a function of K for $a = a_s$ is shown in Fig. 12. It increases slightly as K increases and goes to infinity at $K = 1$, where Eq. (23) is marginally stable.

In a more general way, the nonlinear control with memory for stabilization of an UPO in a one-dimensional map with period m is given by

$$x_{n+m} = F^m(x_n) + \epsilon_n \quad (30)$$

$$\epsilon_{n+m} = -K[F^m(x_{n+m}) - F^m(x_n)] + R\epsilon_n. \quad (31)$$

For the case in which $K = R$ this control reduces to the optimized version

$$x_{n+m} = F^m(x_n) - K[F^m(x_n) - x_n] \quad (32)$$

Also higher periodic orbits the dimensionality of the controlled map is still one. The fixed points of the iterated map are identical to the fixed points of the uncontrolled equation. We have applied the optimized control for a period-two orbit ($m = 2$) of the logistic map, in which the fixed points are given by $x_f = [4a + 1 \pm \sqrt{(4a - 3)(4a + 1)}]/8a$. The eigenvalue for the period-two orbit can be easily calculated and one finds that a pitchfork bifurcation from period-two to period-four will occur when $a^* = \frac{1}{4}[1 + \sqrt{5 + (1 + K)/(1 - K)}]$. The superstable orbit is at $a_s = \frac{1}{4}[1 + \sqrt{5 + K/(1 - K)}]$. The value of a where the bifurcation from period-one to period-two occurs is at $a = 0.75$, which is the same value found in the uncontrolled map. Consequently, the region of the parameter space where control can be achieved in the period-two orbit also grows with increasing K , and goes to infinity as K tends to one. We note that the period-two orbit is also controllable by the methods considered in section II, but are also “non-optimal” in the sense that we have discussed.

Although the results of our study of controlling a simple one-dimensional mapping are suggestive of general underlying principles, they are not generic. A generalization of our “optimized” control scheme for a period-one orbit can be expressed in the following form

$$\mathbf{u}_{n+1} = \mathbf{P}(\mathbf{u}_n, \mathbf{v}_n) + \mathbf{f}, \quad \mathbf{v}_{n+1} = \mathbf{Q}(\mathbf{u}_n, \mathbf{v}_n), \quad (33)$$

where \mathbf{u} is a vector of the variables that are available for observation and \mathbf{v} describes the remaining variables of the dynamical system which are not available or not of interest. The control term operates only on the \mathbf{u} vector and is given by $\mathbf{f} = K[\mathbf{u}_n - \mathbf{P}(\mathbf{u}_n, \mathbf{v}_n)]$. We apply this more general form to a higher-dimensional mapping. For a specific example, we study the Hénon map, which is given by

$$x_{n+1} = 1 + y_n - ax_n^2, \quad y_{n+1} = bx_n. \quad (34)$$

In this map, for $b = 0.3$ (which is the case we consider here), the period one orbit is stable in the interval $-0.1225 \lesssim a \lesssim 0.3671$. The system enters into chaos when $a \gtrsim 1.059$, and the orbit becomes unbounded for $a \gtrsim 1.428$. For this map we can use three types of control: in both variables, only in the x variable or only in the y variable. For the first type of control we have

$$x_{n+1} = 1 + y_n - ax_n^2 - K[1 + y_n - ax_n^2 - x_n], \quad (35)$$

$$y_{n+1} = bx_n - K[bx_n - y_n]. \quad (36)$$

For the second type of control the equations are

$$x_{n+1} = 1 + y_n - ax_n^2 - K[1 + y_n - ax_n^2 - x_n], \quad (37)$$

$$y_{n+1} = bx_n. \quad (38)$$

The third type of control gives

$$x_{n+1} = 1 + y_n - ax_n^2, \quad (39)$$

$$y_{n+1} = bx_n - K[bx_n - y_n]. \quad (40)$$

In all these cases the fixed points are the same as in the uncontrolled Hénon map, and the feedback term vanishes when control is achieved. We have found that the control does not change the lower boundary of the region of stability of the period-one orbit. However, the upper boundary increases as K increases for the three types of forcing. For example, for $K = 0.4$ the period-one orbit bifurcates at $a \approx 1.98, 1.74, 0.49$ for the first, second and third methods, respectively. Thus, different types of control have different regions for which stabilization is possible. For the Hénon map the largest region of control occurs when the x and y variables are controlled simultaneously. The largest Liapunov exponent for the uncontrolled and for the controlled Hénon map is shown in Fig. 13, also for $K = 0.4$. As we see, no superstable orbit exists for any a , for the period-one orbit in the uncontrolled equation with $b = 0.3$. The feedback terms we use to expand the region of stability modifies the location of the most stable orbit but do not create a superstable orbit when one does not exist for any value of a in the uncontrolled equation.

IV. CONCLUSIONS AND DISCUSSION

We have generalized a method introduced by Pyragas [3], used to control an otherwise unstable periodic orbit,

as applied to mappings. The method consists of feeding back a delayed signal with the delay equal to the period to be controlled, done in such a manner that the position of the stabilized orbit in the phase space is not changed. The generalization consists of feeding back the nonlinear mapping signal, rather than a signal linearized around the fixed point. This increases the basin of attraction of the controlled signal and thus decreases the sensitivity to noise. However, the range of parameters for which control can be achieved is limited. An addition to the control procedure, introduced by Socolar *et. al* [5], is to allow memory of all previous periods. This latter procedure was implemented in the mapping parameter, rather than directly into the variables. The method allows an arbitrary range of the parameter in the logistic map to be tracked, but at the expense of a rapidly decreasing the basin of attraction with increasing range of parameter tracking. A generalization of the nonlinear feedback applied to the variables, to include memory, also allows arbitrary tracking of the parameter, with a significantly improved basin of attraction. All of these above control procedures increase the dimensionality of the phase space for a one-dimensional map to two.

For control with memory there are two parameters to be chosen, the control parameter K and the memory parameter R . For the general case, $R \neq K$, there is no superstable orbit. However, for nonlinear control with the choice $R = K$ the superstable orbit is recovered, and, remarkably, the phase space for the controlled logistic map is again one-dimensional. Because we recover the superstable orbit we call this an “optimized” solution.

The control methods we have been considering have in common with OGY the following properties: (a) the fixed points of the controlled map are the same as in the uncontrolled system; (b) the feedback term vanishes in the absence of noise when control is achieved; and (c) one does not need to know the mapping equations in order to apply the control. Unlike OGY, (d) no computer analysis of the system is necessary to apply the control and the methods probably can be applied for fast systems; and (e) knowledge of the location of the unstable periodic orbit is not necessary. For the “optimized” control, (f) the dimensionality of the controlled equations is the same as in the uncontrolled system; (g) the control does not destroy the superstable orbit of the uncontrolled system; while simultaneously, (h) control can be achieved in a very large region of the parameter space; (i) the basin of attraction of the controlled orbit is larger than in the other methods; and, consequently (j) the control is more robust in the presence of noise. However, (k) to achieve control with the parameter values that are deep within the unstable region, the nonlinear transient times to return to the controlled orbit becomes increasingly long.

Although we have only considered the application to mappings, of the various methods of control, the methods are also applicable to continuous systems governed

by ordinary differential equations (ODE's). This was considered in the original paper by Pyragas [3], who applied the linear control to the Roessler, Duffing and Lorenz systems. However, unlike a mapping, a simple delay makes the dimensionality of the system infinite. We can generalize our nonlinear feedback control for the case of ODE's. For the method without memory the $f(t)$ in Eq. (1) is replaced by $f(t) = -K[P(y(t), \mathbf{x}(t)) - P(y(t-\tau), \mathbf{x}(t-\tau))]$, where τ is the period of the UPO. For the nonlinear control with memory Eq. (1) becomes $\frac{dy(t)}{dt} = P(y(t), \mathbf{x}(t)) + \epsilon(t)$, with $\epsilon(t) = -K[P(y(t), \mathbf{x}(t)) - P(y(t-\tau), \mathbf{x}(t-\tau))] + R\epsilon(t-\tau)$. In the case of the "optimized" control we have for the y -equation $\frac{dy(t)}{dt} = (1-K)P(y(t), \mathbf{x}(t)) + K\frac{dy(t-\tau)}{dt}$. We have achieved control of the Roessler system using all of these types of feedback. We are currently investigating which methods give the best performance with respect to the issues that we considered in this paper.

ACKNOWLEDGMENTS

We thank M. A. Lieberman, J. Socolar and H-A. Tanaka for fruitful discussions. This work was partially supported by the Office of Naval Research (Grant N00014-89-J-1097).

* Electronic address: mariav@eecs.berkeley.edu

- [1] E. A. Jackson, A. W. Huebler, *Physica D*, **44**, 407 (1990).
- [2] E. Ott, C. Grebogi and Y. A. Yorke, *Phys. Rev. Lett.* **64**, 1196 (1990).
- [3] K. Pyragas, *Phys. Lett. A* **170**, 421 (1992).
- [4] K. Pyragas and A. Tamasevicius, *Phys. Lett. A* **180**, 99 (1993).
- [5] J. E. S. Socolar, D. W. Sukow, and D. J. Gauthier, *Phys. Rev. E*, **50**, 3245 (1994).
- [6] D. P. Lathrop and E. J. Kostelich, *Phys. Rev. A* **40**, 4028 (1989).
- [7] S. Bielawski, D. Derozier and P. Glorieux, *Phys. Rev. E*, **49**, R971 (1994).

FIG. 1. Block diagram for the nonlinear feedback control of chaos without memory.

FIG. 2. Boundary of stability of the period-one orbit for the nonlinear control method without memory (solid line) and Pyragas' linear control (dashed line).

FIG. 3. Liapunov exponent, $\log_2 |\lambda|$, as a function of a for the nonlinear control method without memory (solid line) with $K = 1/3$ (the value of K that gives the maximum a^*), Pyragas' linear control (dashed line) along the dotted line of Fig. 2, and for the uncontrolled logistic map (short-dashed line).

FIG. 4. (a) Basin of attraction and noise circle for (a) the nonlinear control without memory for $a = 1$ and $K = 1/3$ and for (b) Pyragas' linear control for $a = 1$ and $K = 0.75$.

FIG. 5. Noise radius r as a function of a for the nonlinear control method at $K = 1/3$ (solid line) and for Pyragas' linear control along the dotted line of Fig. 2 (dashed line).

FIG. 6. Boundary of stability for the period-one orbit using our nonlinear control method with memory (solid line) and Socolar's control method (dashed line), with $R = 0.5$ in both cases.

FIG. 7. Basin of attraction and noise circle for (a) our nonlinear control with memory at $K = 0.6428$, and (b) for Socolar's control method at $K = 1.8333$. In both cases, $R = 0.5$ and $a = 1$. These parameters correspond to the diamond symbol and cross shown in Fig. 6.

FIG. 8. Rescaled noise radius r as a function of a for our nonlinear control with memory with $K = 0.6428$ (that is, the value of K that gives the maximum a^* in Fig. 6), and Socolar's control method along the median line of the boundary of stability shown in Fig. 6. In both cases $R = 0.5$.

FIG. 9. Block diagram for our optimal control method.

FIG. 10. a^* and a_s for the logistic map using the optimal control method.

FIG. 11. Liapunov exponent, $\log_2 |\lambda|$, for $K = 0$ (solid line), $K = 0.4$ (dashed line), and $K = 0.8$ (long-dashed line) for the logistic map using the optimal control method.

FIG. 12. Nonlinear transient for the logistic map along the line of the superstable orbit, a_s , shown in Fig. 9.

FIG. 13. The largest Liapunov exponent, $\log_2 |\lambda|$, for the Hénon map without feedback (label 'Henon'), with feedback in the x and y variables (label 'xy'), with feedback only in the x variable (label 'x'), and with feedback only in the y variable (label 'y').

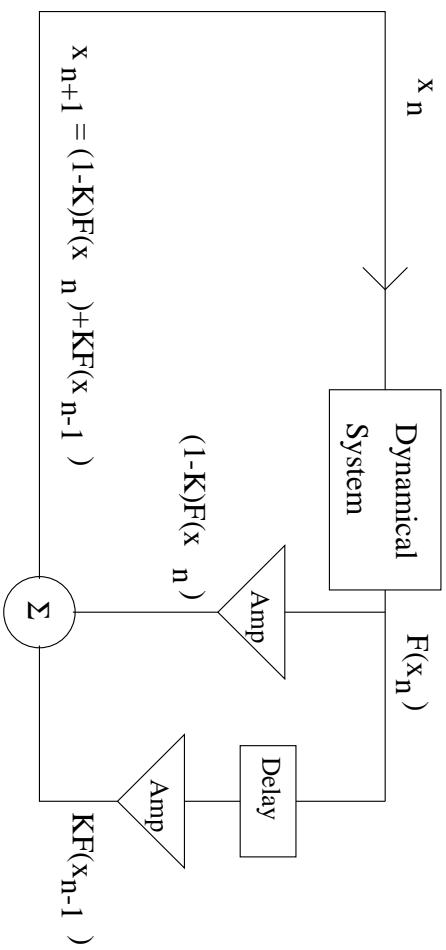


Fig. 1

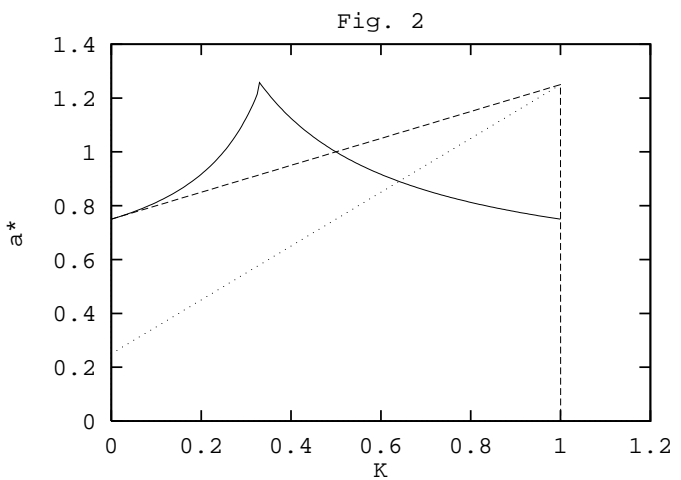


Fig. 2

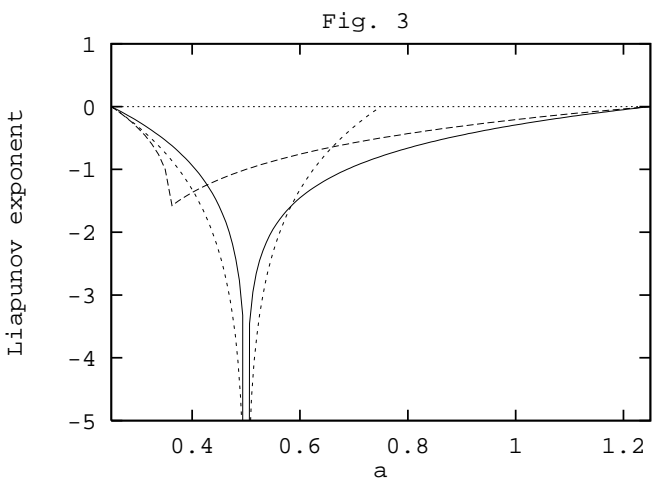
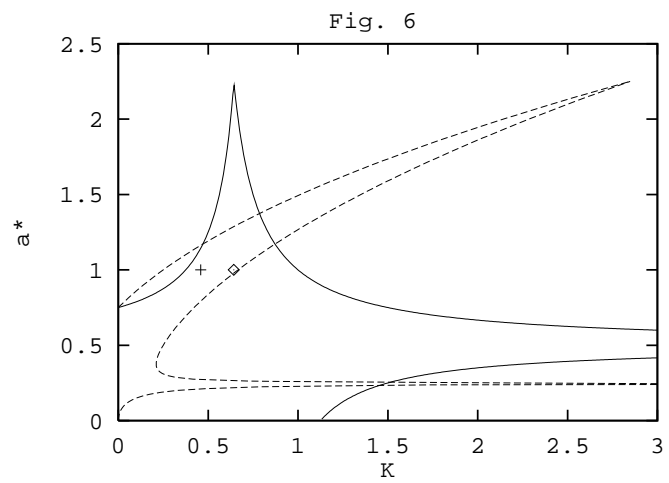
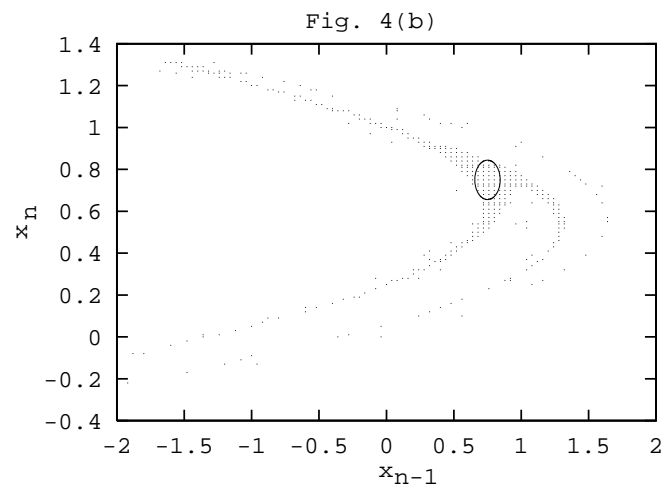
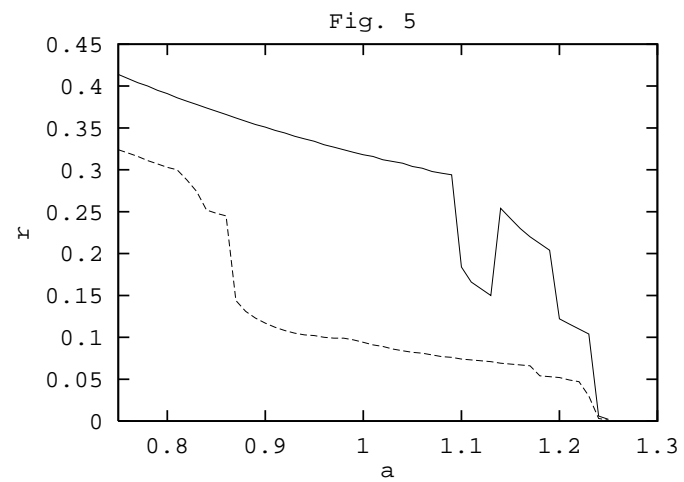
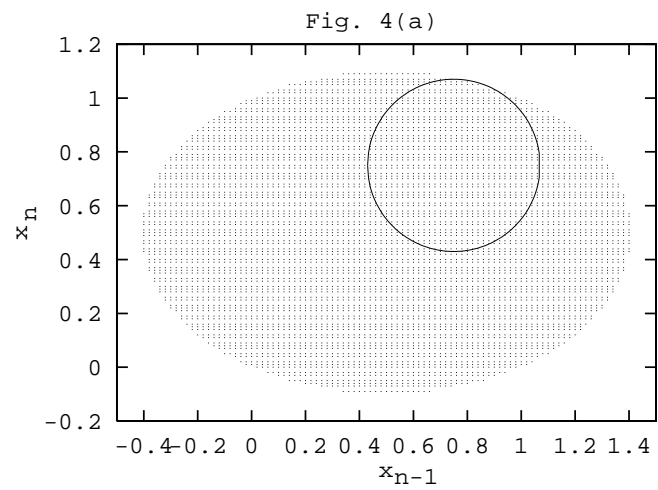
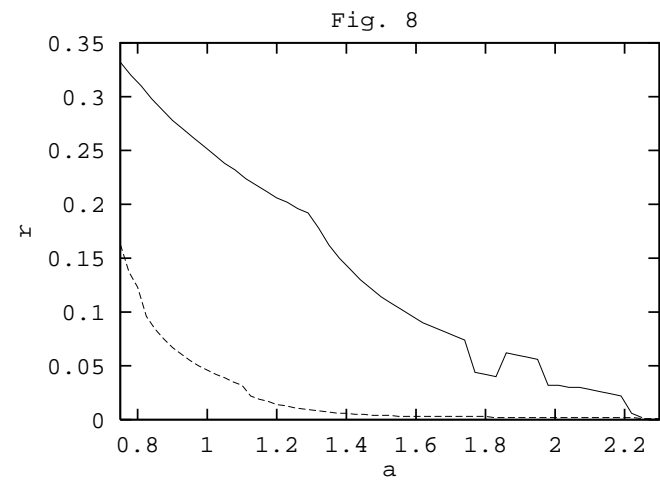
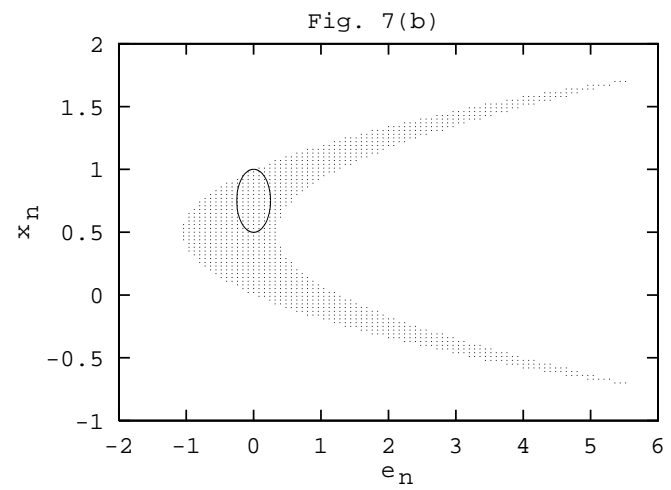
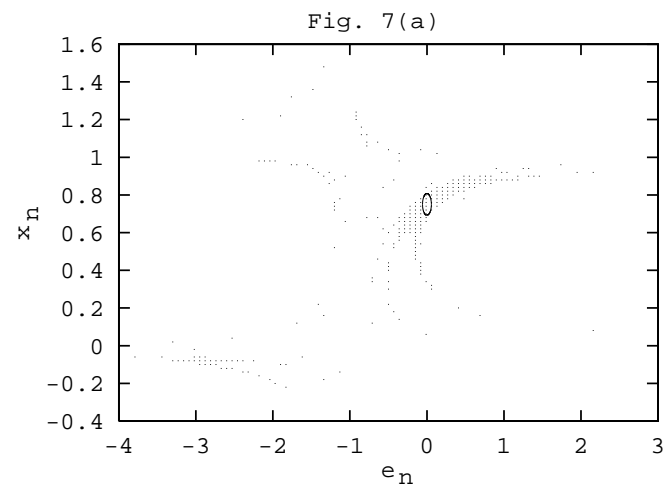


Fig. 3





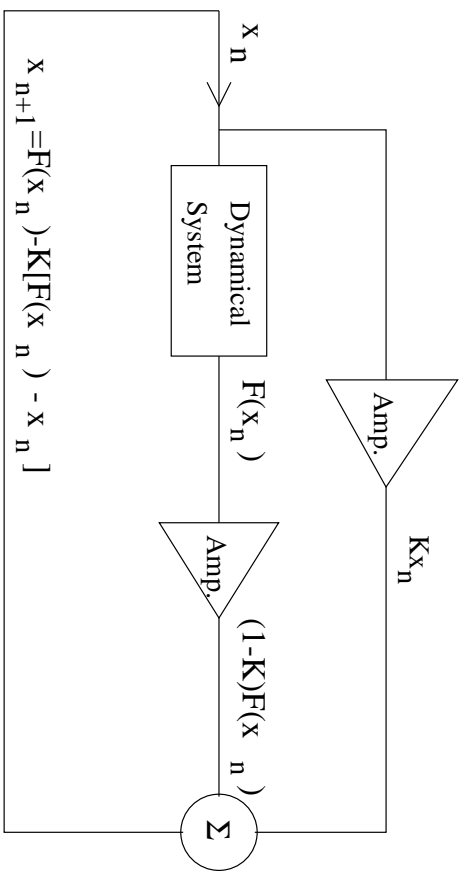


Fig. 9

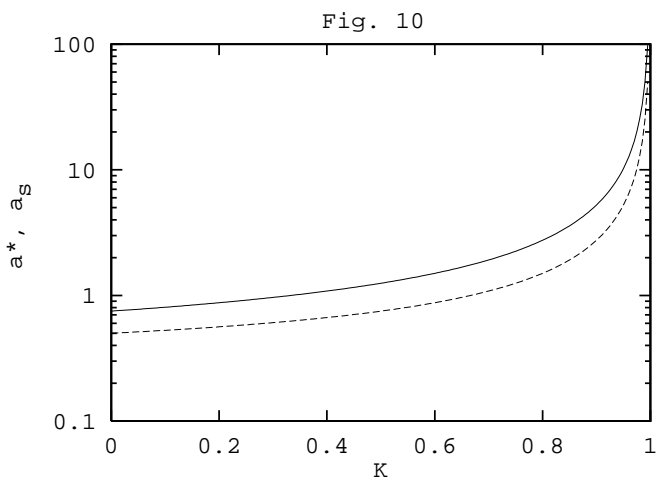


Fig. 10

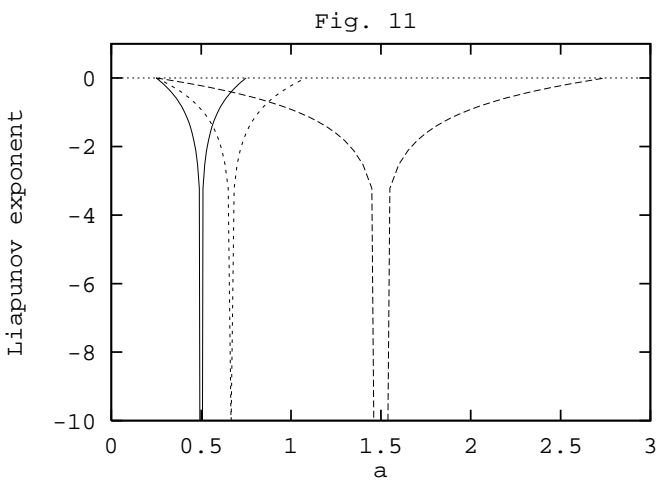


Fig. 11

Fig. 12

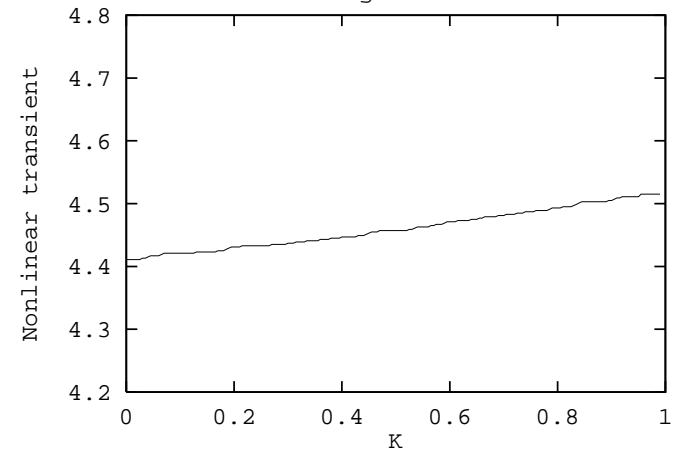


Fig. 13

